JOINT EUROPEAN TORUS

JET–P(89)04

A. Boileau, M. von Hellerrnann, W. Mandl, H.P. Summers,
H. Weisen and A. Zinoviev and JET Team

Observations of Motional Stark Features in the Balmer Spectrum of Deuterium in the JET Plasma

Observations of Motional Stark Features in the Balmer Spectrum of Deuterium in the JET Plasma

A. Boileau[1], M. von Hellerrnann, W. Mandl, H.P. Summers,
H. Weisen and A. Zinoviev[2] and JET Team*

JET-Joint Undertaking, Culham Science Centre, OX14 3DB, Abingdon, UK

[1]Tokamak de Varennes, Quebec, CANADA
[2]Ioffe Institute, Leningrad, USSR
** See Appendix 1*

Preprint of Paper to be submitted for publication in
Journal of Physics B

OBSERVATIONS OF MOTIONAL STARK FEATURES IN THE BALMER SPECTRUM OF DEUTERIUM IN THE JET PLASMA

A Boileau+, M von Hellermann, W Mandl, H P Summers, H Weisen and A Zinoviev*

JET Joint Undertaking, Abingdon, Oxon OX14 3EA, UK
+ Tokamak de Varennes, Quebec, CANADA
* Permanent address: Ioffe Institute, Leningrad, USSR

ABSTRACT

Observations are reported of resolved components of deuterium Balmer emission in neutral beam heated JET plasmas. The features are interpreted as Doppler shifted emission from deuterium in the neutral beams spectrally resolved into components by the $\underline{v} \times \underline{B}$ motional Stark electric field. The mechanisms of excitation of the deuterium are elucidated and the emission modelled. Attention is drawn to the diagnostic potential of the observations for measurement of local magnetic fields, deuteron density and effective plasma ion charge.

1. INTRODUCTION

The Joint European Torus (JET) is a fusion research device of tokamak design. In its present configuration, it can sustain a multi-keV deuterium plasma for up to 20 secs at densities $\sim 5\times10^{13}$ cm^{-3}. The ohmic heating of the plasma by the induced toroidal current ($I_p \leq 6$ MA) is supplemented by ion cyclotron resonance heating (ICRH power ≤ 24 MW) and neutral deuterium beam injection (NBI power ≤ 21 MW). The NBI system consists of two boxes on either side of the torus which are equipped with eight sources each. The primary deuterium energy is 40 keV/amu. A spectroscopic diagnostic system has been implemented to exploit the emission in the visible following

charge transfer reactions between neutral beam particles and thermal plasma ions (Boileau et al., 1989) for ion temperature, density and plasma rotation profiles. The spatial arrangement is shown in figure 1. (B) is a single vertical line-of-sight intersecting one of the neutral beam lines and (A) represents a nearly horizontal fan of 15 viewing lines intersecting the beam line at various radial positions, R (measured from the central axis in the horizontal section) and angles, θ (measured relative to the -ve beam direction).

The spectrum in the vicinity of deuterium Balmer α (6560 A) during the NBI phase of JET pulse #14825 is shown in figure 2. The viewing line used for this spectrum intersects the neutral beam with θ = 134° and at a toroidal major radius R = 369 cm (plasma centre is at ~ 312 cm). The complex spectral structure is associated with a combination of plasma deuterium and neutral beam deuterium emission and separates into three main parts. (A) is principally a cold edge feature, corresponding to a deuterium temperature $T_D^{(A)}$ ~ 40 eV, which is also present before the neutral beams are switched on. Higher resolution measurement (see insert from pulse #17719) reveals it to be a partially filled Zeeman doublet appropriate to the viewing line/magnetic field inclination at the vessel wall. Prior to beam switch on, the wings of this feature indicate the presence of an underlying broad 'pedestal' (equivalent T_D ~ 800 eV). This is believed to have its origin in and reflect the temperature of the plasma layers fairly close to the limiting surfaces. Neutral deuterium recycling from limiters penetrates approximately 10 cm into the plasma due to resonant charge transfer with plasma deuterons. Feature (B) is present only with the beams and is the primary charge exchange feature at the beam/plasma/viewing line intersection. In this case $T_D^{(B)}$ ~ 2.7 keV. However the feature is revealed to be asymmetric with the blue wing enhanced. This and the necessity of subtracting the 40 eV and 800 eV features limits the precision of the temperature derivation. The asymmetry is principally due to the favouring of charge transfer to plasma deuterons comoving

with the beam because of the rapid fall of the charge exchange cross sections for relative velocity $v > 1.5\ v_o$ (v_o is the Bohr orbital speed ≡ 25 keV/amu). The features (C) are Doppler shifted emission from the deuterium in the beam. The three subfeatures (C_1, C_2, C_3) are associated with the full, half and third energy components in the beam arising from molecular ions in the source. Each subfeature is resolved into Stark components of π and σ polarisation by the Lorentz field $|\underline{E}| = |\underline{v} \times \underline{B}|$ ~ 0.48×10^5 V/cm caused by the cross-field motion of the beam particles ($v \sim 2.8 \times 10^6$ cm/sec, B ~ 2.3 Tesla). The full energy feature (C_1) is shown in figure 3 for another pulse at higher magnetic field (B ~ 3.2 Tesla) and higher spectral resolution to resemble a 'textbook' description (Bethe & Salpeter, 1958).

It is found that the ratio of emissions in features C and B is almost independent of the toroidal minor radius but depends upon the purity of the plasma with $\frac{I_C}{I_B}$ large for large Z_{eff}. Z_{eff} is defined as $(N_D + \sum_i Z_i^2 N_i)/N_e$ with the sum over impurity species of number density N_i and nuclear charge Z_i. N_D is the deuteron density and N_e the electron density. The absolute Doppler shifts and the absolute intensities of features C_1, C_2, C_3 vary across the poloidal radius (reflecting the varying angle θ, and beam attenuation). The subfeature compression and ratio of σ to π components also vary with radius. An equivalent structure is observed in Balmer β. There is substantial diagnostic advantage to be gained for tokamak plasma interpretation from analysis of these spectral features and their behaviour. Parameters which are accessible include poloidal magnetic field, plasma paramagnetism, neutral beam attenuation, Z_{eff}, excited deuterium corrections to charge exchange recombination spectroscopy, plasma deuteron temperature and density. This is revealed on detailed modelling.

2. MODELLING OF THE EMISSION

The spectrum has been fitted by a multiple Gaussian constrained to equally spaced Stark features. The component wavelength

separation and the intensity ratio of the σ and π components in principle enable the deduction of the local magnetic field and its orientation in space.

The magnetic field in a tokamak is dominated by the externally applied component around the major axis of the torus (the toroidal direction). The plasma current primarily flows toroidally and generates a magnetic field in the minor (or poloidal) direction. The toroidal magnetic field is modified by paramagnetism and diamagnetism. The former arises because the plasma current mainly flows along the magnetic field and so picks up a poloidal component. The diamagnetism is a result of the slight deviation of the plasma current from the direction of the magnetic field which is required to balance the plasma thermal pressure. The paramagnetism increases the toroidal magnetic field and the diamagnetism decreases it. In a tokamak like JET, both corrections can be as much as 10%.

For the present observational geometry, the induced Lorentz field is almost orthogonal to the viewing directions ($85° < \psi < 100°$) which implies that the intensity ratio of σ and π components is insensitive to changes of the total field orientation. The experimental results of wavelength separation of Stark components (statistical errors typically less than 1%) can however be used in conjunction with toroidal field and flux surface data from equilibrium calculations to derive a poloidal field profile. Analysis indicates that in this case the dominant error sources are the data on the toroidal field (including paramagnetic and diamagnetic contributions) and that of the flux geometry. It is evident that the present neutral beam orientation and viewing line directions are not ideal for poloidal field deduction.

Full intensity simulation is required to exploit the π and σ observed ratios and to allow deduction of the other plasma parameters summarised earlier.

The Stark state energy levels and transition probabilities have been examined by a number of authors (Isler, 1976; Breton et al., 1980; Souw & Uhlenbusch, 1983). Diagonalising of the isolated hydrogen atom Hamiltonian perturbed by magnetic moment $\underline{\mu}.\underline{B}$ and motional electric field $e\,\underline{v} \times \underline{B}.\underline{r}$ terms yields essentially a Stark energy level pattern (basic interval 3.03 cm^{-1} at $v = 1.27\ v_o$, $B = 1.74$ Tesla, and $v \perp B$). The Zeeman contribution is ~ 10% of the Stark and since the magnetic field is orthogonal to the Stark electric field does not resolve further the residual D_α multiplet degeneracy. Plasma radial electric fields play a negligible role.

The relative collision speed for deuterium atoms in the beam is dominated by the beam speed for collisions with plasma ions and by the Maxwellian electron speeds for collisions with electrons. Collisions of the former type dominate for $E_{beam} \geq$ 25 keV/amu - the situation here. This is shown in the comparative figure 4 for the total excitation cross-sections from D(1s)→D(n=3). The cross-sections for excitation and ionisation by ions of different charge z, but the same collision speed ($\geq 1\ v_o$) are approximately proportional to z^2. Therefore Z_{eff} provides the appropriate weighting of the deuteron impact excitation rate to account for impure plasmas.

Since the positive ion collisions are essentially monodirectional and monoenergetic with oriented Stark states, the fractional m-subshell selective collision cross-sections between different n-shells have been calculated in a first Born approximation using the Stark/Zeeman eigenfunctions. For axis of quantisation nearly orthogonal to the beam direction and beam energy relevant here, the selective directional effect is not large but rather the field induced state mixings are most important.

The complete population structure of the excited deuterium states has been modelled with full Stark/Zeeman state resolution for $1 \leq n \leq 4$ and bundle-n resolution for $4 < n \leq 10$. Ion impact dominates for both excitation and ionisation. The collision

limit approaches n=4 at typical JET densities. Stepwise ionisation, de-excitation collisions and redistributing collisions amongst nearly degenerate states are all active. Figure 5 illustrates the calculated relative emissivities of the Balmer α components as a function of density. Notable is the development of the 0^0 component which partly arises from the parabolic upper states (0,0, ± 2). These states are accessible only by redistributive collisions and cascade rather than by direct excitation from the ground state. The populations are strongly density sensitive in the range 10^{12} to 10^{14} cm^{-3} due to the encroachment of the collision limit on the n=4, 3 levels. The theoretical effective emission coefficients for the summed Dα and Dβ transition arrays are approximately in the ratio 8:1 and increase linearly with Z_{eff} for Ne $\leq 10^{13}$ cm^{-3}. The coefficients are approximately constant with density for Ne $>10^{12}$ cm^{-3}. The coefficients for different Z_{eff} converge at high density.

In simulating observed π and σ components the usual $\sin^2\psi$, $\frac{1}{2}(1+\cos^2\psi)$ polar dependence on viewing line/electric field angle, ψ must be taken into account. The simulated pattern is also modified by the polarisation selective reflection characteristics of the collection optics. Figure 6 gives a comparison of the measured and calculated primary Stark features for a set of radial positions for JET pulse #16018. The 'experimental' data shown is the full beam energy Stark components isolated by fitting Gaussian profiles to the complete set of Balmer α features as described earlier. The fitting is very precise and reliable for the Stark components with no asymmetries indicated. The displayed full energy data is therefore a faithful representation of that part of the raw data. Relative calibration of viewing lines was initially sought by measuring the underlying bremsstrahlung background and assuming constant Zeff radially across the plasma. This assumption is based on the observed approximate constancy of the charge exchange to Stark features for the pulse at the indicated time. The statistical error on the bremsstrahlung measurement at R=349 cm was very large. A discrepancy

(≃ factor 2) was also evident on this track on comparing intensities with beam attenuation calculations radially. The inferred adjustments for other tracks were much smaller ($\lesssim$30%). The experimental data displayed include these adjustments. The instrument width has also been deconvolved. Observed Doppler shifts indicated viewing line/beam intersection positions in agreement with those physically measured to <.5%. The deduced total magnetic field from component separation was combined with the toroidal field from equilibrium calculation to yield the poloidal field as shown. The safety factor on axis $q = (B_T/R_o)/(\partial B_p/\partial r)$ derived from the slope of $B_p(R)$ is within 6% of the equilibrium value.

The theoretical figures are based on the calculated beam attenuation, deduced magnetic induction B, measured viewing lines, measured reflection characteristic of the metal mirror in the collection optical chain and measured electron temperature and density profiles. The theoretical components have been given Gaussian profiles corresponding to a temperature of 12 eV. This temperature is not real but describes the beam divergence. The relative intensities of theory and experiment are in agreement to within ~50%. The σ/π component ratio comparison indicates that the reflection effect on the polarisation for the innermost viewing line is underestimated by ~30%.

3. CONCLUSIONS

The observations shown here, though 'classical' in their structure are believed to be unique. The principal collisional phenomena involved in exciting the observed spectrum have been identified although the model/experiment matching remains at this stage semiquantitative.

The diagnostic implications for JET are very large. The measurements are not only of localised emitting regions in space (so requiring no Abel inversion) but also use a restricted, easily observed and calibrated spectral region. It has been shown that parameters of the internal tokamak magnetic

fields can be deduced. This is a most important capability for which there are few alternatives.

Z_{eff} deduction is particularly promising since it is not only likely to be very sensitive (since the charge exchange feature decreases with dilution and the Stark feature increases with Z_{eff}), but also because it is calibration independent.

The observation will allow greater precision in charge exchange recombination spectroscopy of impurities in JET since beam attenuation and excited deuterium content of the beam can be measured and used self consistently. Deuteron temperature and density in the plasma will also be obtainable.

A full description of the observations and the model and their confrontation will be published in due course.

ACKNOWLEDGEMENT

We are grateful to Dr's J O'Rourke and E Lazzaro for providing the equilibrium magnetic calculation and to Dr P Thomas for helpful discussion.

HPS is on secondment from Strathclyde University.

REFERENCES

H A Bethe & E E Salpeter(1958) 'Quantum Mechanics of One and Two Electron Atoms (publ. Springer-Verlag).

A Boileau, M von Hellermann, L D Horton, J Spence and H P Summers (1989) Plasma Physics & Controlled Fusion - in press (JET Joint Undertaking report JET-P(87)44)

C Breton, C de Michelis, M Finkenthal and M Mattioli (1980) J. Phys. B 13, 1703.

W Fritsch and C D Lin (1983) Phys. Rev. A 27, 3361.

R C Isler (1976) Phys. Rev. A 14, 1015.

J T Park, J E Alday, J M George, J L Peacher (1976) Phys. Rev. A 14, 608.

R Shakeshaft (1979) Phys. Rev. A 18, 1930.

E K Souw and J Uhlenbusch (1983) Physica 122C, 353.

FIG 2

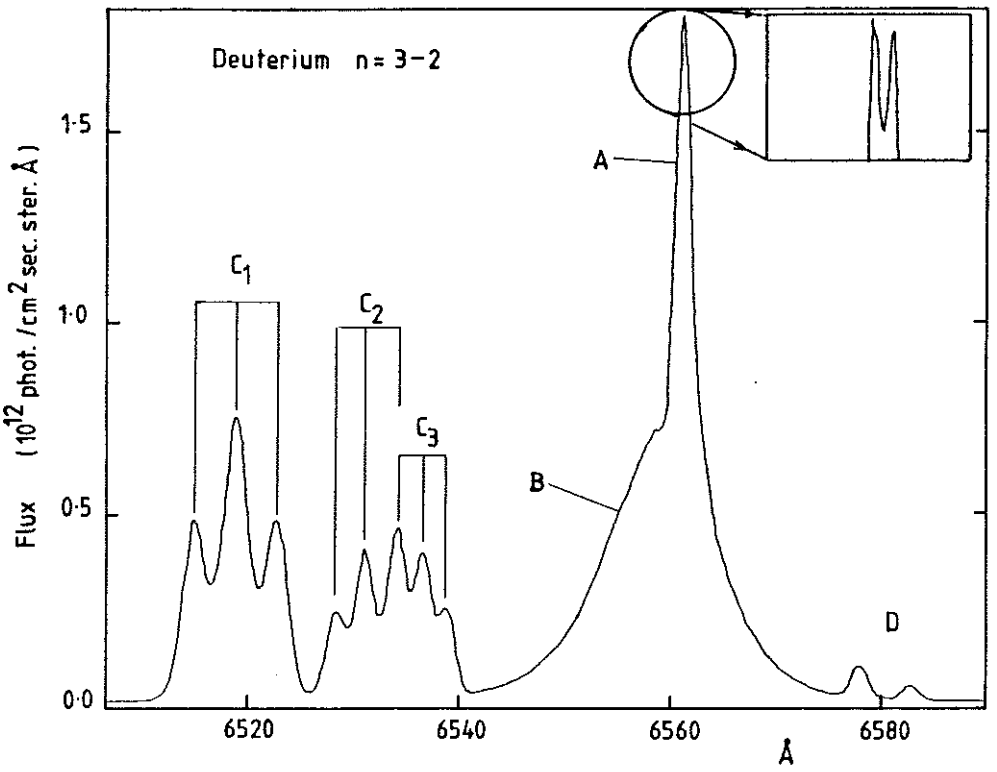
Deuterium n = 3–2
Flux (10^12 phot. /cm^2 sec. ster. Å)
1·5
1·0
0·5
0·0
C1
C2
C3
A
B
D
6520
6540
6560
6580
Å

FIG 3

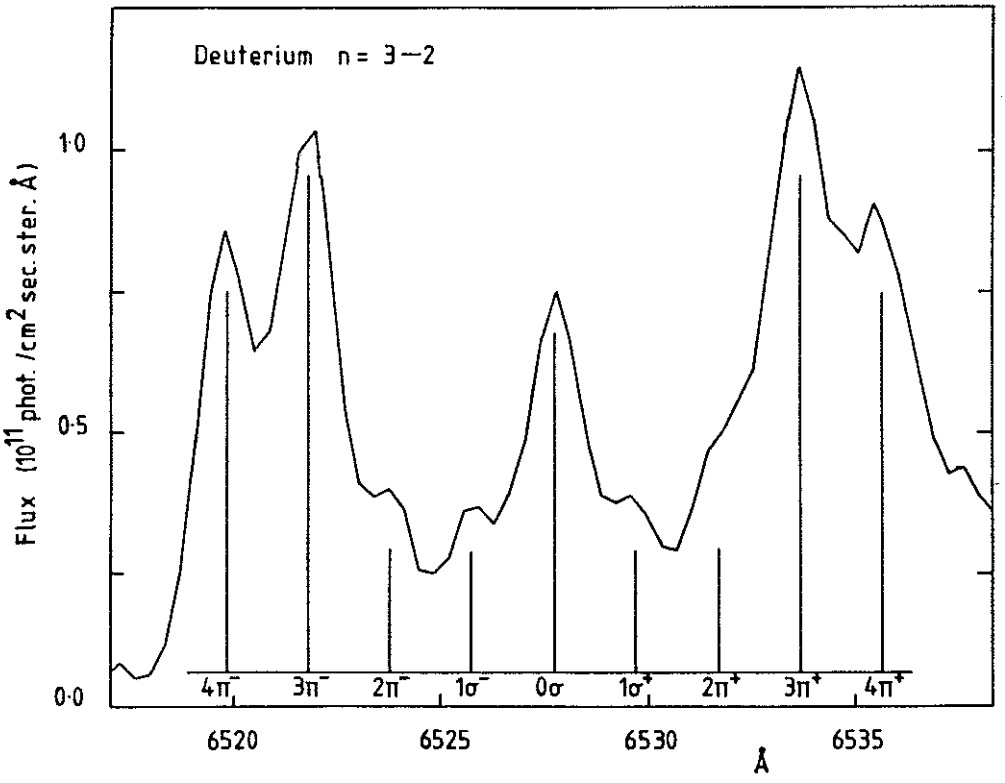
Deuterium n = 3—2
Flux (10^11 phot. /cm^2 sec. ster. Å)
1·0
0·5
0·0
4π⁻
3π⁻
2π⁻
1σ⁻
0σ
1σ⁺
2π⁺
3π⁺
4π⁺
6520
6525
6530
6535
Å

FIG 4

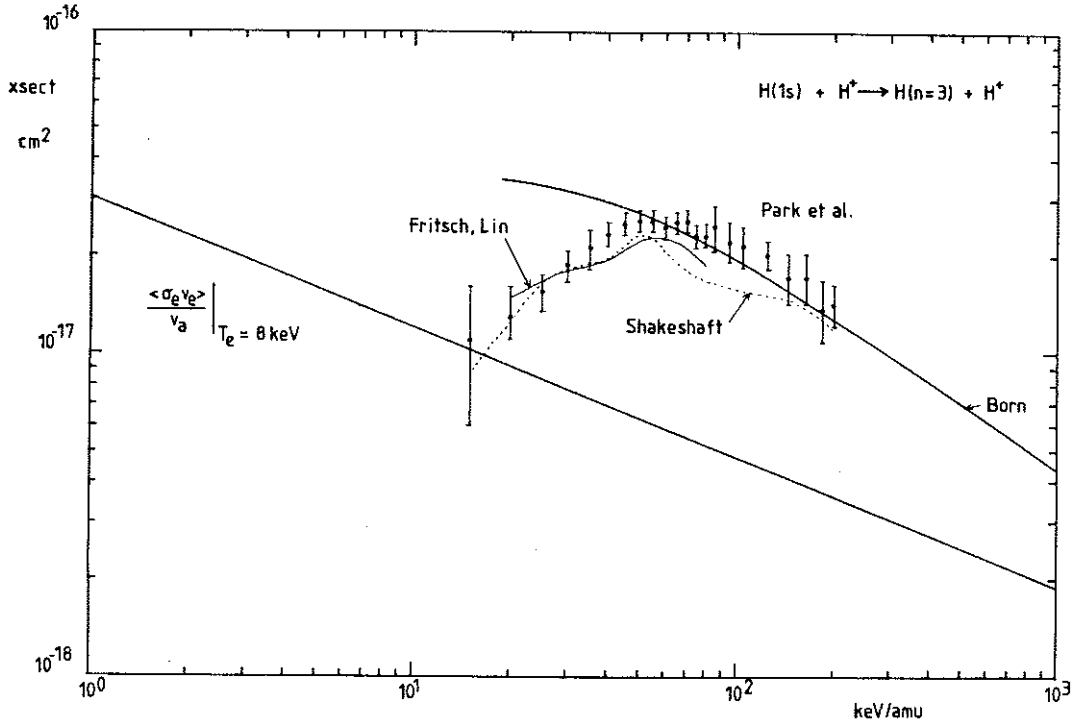
xsect
cm2
H(1s) + H+ → H(n=3) + H+
Fritsch, Lin
Park et al.
Shakeshaft
Born
Te = 8 keV
keV/amu

FIG 5

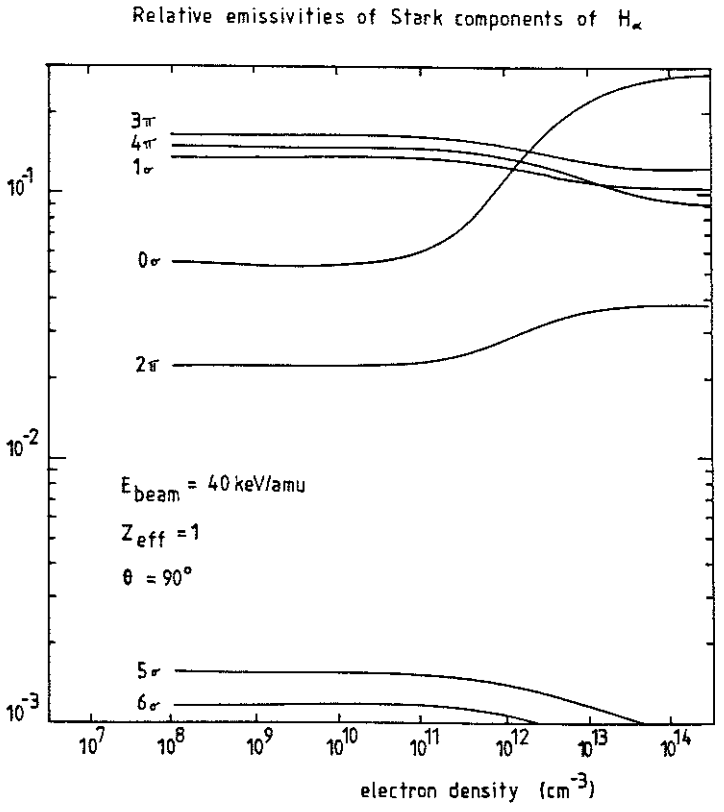
Relative emissivities of Stark components of Hα
3π
4π
1σ
0σ
2π
Ebeam = 40 keV/amu
Zeff = 1
θ = 90°
5σ
6σ
electron density (cm-3)

FIG 6

Comparison of experiment and theory for full energy Stark features.
JET pulse = 16018 at 15·38 sec.

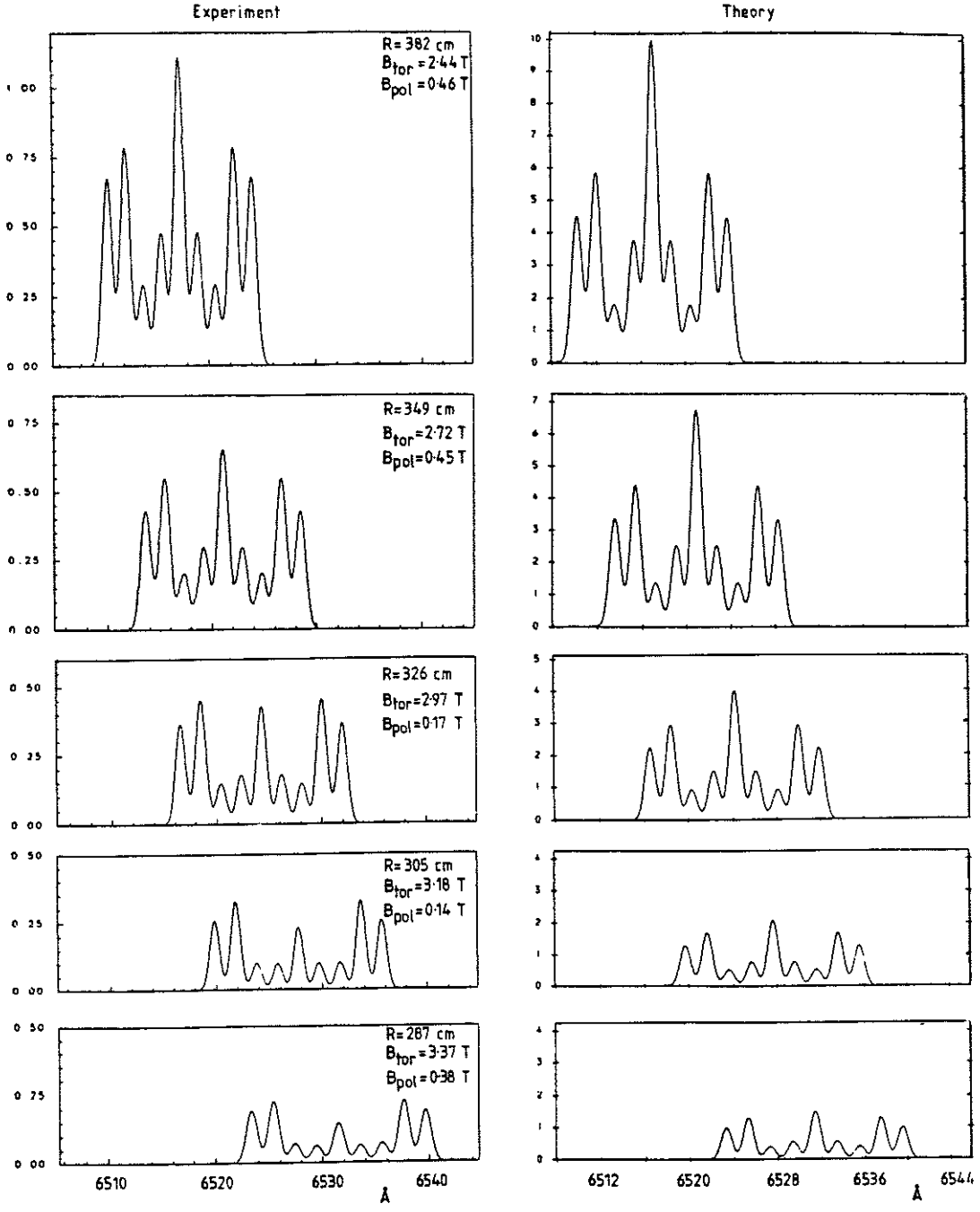

APPENDIX 1.

THE JET TEAM

JET Joint Undertaking, Abingdon, Oxon, OX14 3EA, U.K.

J.M.Adams[1], F.Alladio[4], H.Altmann, R.J.Anderson, G.Appruzzese, W.Bailey, B.Balet, D.V.Bartlett, L.R.Baylor[24], K.Behringer, A.C.Bell, P.Bertoldi, E.Bertolini, V.Bhatnagar, R.J.Bickerton, A.Boileau[3], T.Bonicelli, S.J.Booth, G.Bosia, M.Botman, D.Boyd[31], H.Brelen, H.Brinkschulte, M.Brusati, T.Budd, M.Bures, T.Businaro[4], H.Buttgereit, D.Cacaut, C.Caldwell-Nichols, D.J.Campbell, P.Card, J.Carwardine, G.Celentano, P.Chabert[27], C.D.Challis, A.Cheetham, J.Christiansen, C.Christodoulopoulos, P.Chuilon, R.Claesen, S.Clement[30], J.P.Coad, P.Colestock[6], S.Conroy[13], M.Cooke, S.Cooper, J.G.Cordey, W.Core, S.Corti, A.E.Costley, G.Cottrell, M.Cox[7], P.Cripwell[13], F.Crisanti[4], D.Cross, H.de Blank[16], J.de Haas[16], L.de Kock, E.Deksnis, G.B.Denne, G.Deschamps, G.Devillars, K.J.Dietz, J.Dobbing, S.E.Dorling, P.G.Doyle, D.F.Düchs, H.Duquenoy, A.Edwards, J.Ehrenberg[14], T.Elevant[12], W.Engelhardt, S.K.Erents[7], L.G.Eriksonn[5], M.Evrard[2], H.Falter, D.Flory, M.Forrest[7], C.Froger, K.Fullard, M.Gadeberg[11], A.Galetsas, R.Galvao[8], A.Gibson, R.D.Gill, A.Gondhalekar, C.Gordon, G.Gorini, C.Gormezano, N.A.Gottardi, C.Gowers, B.J.Green, F.S.Griph, M.Gryzinski[26], R.Haange, G.Hammett[6], W.Han[9], C.J.Hancock, P.J.Harbour, N.C.Hawkes[7], P.Haynes[7], T.Hellsten, J.L.Hemmerich, R.Hemsworth, R.F.Herzog, K.Hirsch[14], J.Hoekzema, W.A.Houlberg[24], J.How, M.Huart, A.Hubbard, T.P.Hughes[32], M.Hugon, M.Huguet, J.Jacquinot, O.N.Jarvis, T.C.Jernigan[24], E.Joffrin, E.M.Jones, L.P.D.F.Jones, T.T.C.Jones, J.Källne, A.Kaye, B.E.Keen, M.Keilhacker, G.J.Kelly, A.Khare[15], S.Knowlton, A.Konstantellos, M.Kovanen[21], P.Kupschus, P.Lallia, J.R.Last, L.Lauro-Taroni, M.Laux[33], K.Lawson[7], E.Lazzaro, M.Lennholm, X.Litaudon, P.Lomas, M.Lorentz-Gottardi[2], C.Lowry, G.Magyar, D.Maisonnier, M.Malacarne, V.Marchese, P.Massmann, L.McCarthy[28], G.McCracken[7], P.Mendonca, P.Meriguet, P.Micozzi[4], S.F.Mills, P.Millward, S.L.Milora[24], A.Moissonnier, P.L.Mondino, D.Moreau[17], P.Morgan, H.Morsi[14], G.Murphy, M.F.Nave, M.Newman, L.Nickesson, P.Nielsen, P.Noll, W.Obert, D.O'Brien, J.O'Rourke, M.G.Pacco-Düchs, M.Pain, S.Papastergiou, D.Pasini[20], M.Paume[27], N.Peacock[7], D.Pearson[13], F.Pegoraro, M.Pick, S.Pitcher[7], J.Plancoulaine, J-P.Poffé, F.Porcelli, R.Prentice, T.Raimondi, J.Ramette[17], J.M.Rax[27], C.Raymond, P-H.Rebut, J.Removille, F.Rimini, D.Robinson[7], A.Rolfe, R.T.Ross, L.Rossi, G.Rupprecht[14], R.Rushton, P.Rutter, H.C.Sack, G.Sadler, N.Salmon[13], H.Salzmann[14], A.Santagiustina, D.Schissel[25], P.H.Schild, M.Schmid, G.Schmidt[6], R.L.Shaw, A.Sibley, R.Simonini, J.Sips[16], P.Smeulders, J.Snipes, S.Sommers, L.Sonnerup, K.Sonnenberg, M.Stamp, P.Stangeby[19], D.Start, C.A.Steed, D.Stork, P.E.Stott, T.E.Stringer, D.Stubberfield, T.Sugie[18], D.Summers, H.Summers[20], J.Taboda-Duarte[22], J.Tagle[30], H.Tamnen, A.Tanga, A.Taroni, C.Tebaldi[23], A.Tesini, P.R.Thomas, E.Thompson, K.Thomsen[11], P.Trevalion, M.Tschudin, B.Tubbing, K.Uchino[29], E.Usselmann, H.van der Beken, M.von Hellermann, T.Wade, C.Walker, B.A.Wallander, M.Walravens, K.Walter, D.Ward, M.L.Watkins, J.Wesson, D.H.Wheeler, J.Wilks, U.Willen[12], D.Wilson, T.Winkel, C.Woodward, M.Wykes, I.D.Young, L.Zannelli, M.Zarnstorff[6], D.Zasche[14], J.W.Zwart.

PERMANENT ADDRESS

1. UKAEA, Harwell, Oxon. UK.
2. EUR-EB Association, LPP-ERM/KMS, B-1040 Brussels, Belgium.
3. Institute National des Récherches Scientifique, Quebec, Canada.
4. ENEA-CENTRO Di Frascati, I-00044 Frascati, Roma, Italy.
5. Chalmers University of Technology, Göteborg, Sweden.
6. Princeton Plasma Physics Laboratory, New Jersey, USA.
7. UKAEA Culham Laboratory, Abingdon, Oxon. UK.
8. Plasma Physics Laboratory, Space Research Institute, Sao José dos Campos, Brazil.
9. Institute of Mathematics, University of Oxford, UK.
10. CRPP/EPFL, 21 Avenue des Bains, CH-1007 Lausanne, Switzerland.
11. Risø National Laboratory, DK-4000 Roskilde, Denmark.
12. Swedish Energy Research Commission, S-10072 Stockholm, Sweden.
13. Imperial College of Science and Technology, University of London, UK.
14. Max Planck Institut für Plasmaphysik, D-8046 Garching bei München, FRG.
15. Institute for Plasma Research, Gandhinagar Bhat Gujat, India.
16. FOM Instituut voor Plasmafysica, 3430 Be Nieuwegein, The Netherlands.
17. Commissiariat à L'Energie Atomique, F-92260 Fontenay-aux-Roses, France.
18. JAERI, Tokai Research Establishment, Tokai-Mura, Naka-Gun, Japan.
19. Institute for Aerospace Studies, University of Toronto, Downsview, Ontario, Canada.
20. University of Strathclyde, Glasgow, G4 ONG, U.K.
21. Nuclear Engineering Laboratory, Lapeenranta University, Finland.
22. JNICT, Lisboa, Portugal.
23. Department of Mathematics, Univeristy of Bologna, Italy.
24. Oak Ridge National Laboratory, Oak Ridge, Tenn., USA.
25. G.A. Technologies, San Diego, California, USA.
26. Institute for Nuclear Studies, Swierk, Poland.
27. Commissiariat à l'Energie Atomique, Cadarache, France.
28. School of Physical Sciences, Flinders University of South Australia, South Australia SO42.
29. Kyushi University, Kasagu Fukuoka, Japan.
30. Centro de Investigaciones Energeticas Medioambientales y Techalogicas, Spain.
31. University of Maryland, College Park, Maryland, USA.
32. University of Essex, Colchester, UK.
33. Akademie de Wissenschaften, Berlin, DDR.

CR 88.49.1A